Hindawi
Geofluids
Volume 2020, Article ID 9742142, 8 pages
https://doi.org/10.1155/2020/9742142

Research Article

The Experimental Investigation of the Development Potential of Low-Permeability Reservoirs in the Daqing Oilfield

Yazhou Zhou[1,2] **and Daiyin Yin**[1,2]

[1]*Department of Petroleum Engineering, Northeast Petroleum University, Daqing, China*
[2]*Key Laboratory of Enhanced Oil Recovery (Northeast Petroleum University), Ministry of Education, Daqing, China*

Correspondence should be addressed to Daiyin Yin; yindaiyin@nepu.edu.cn

Received 29 December 2019; Revised 8 May 2020; Accepted 12 May 2020; Published 29 May 2020

Academic Editor: Zhenjiang You

It is very risky and difficult to develop low-permeability reservoirs, but reservoir development can be guided by the development potential of different low-permeability reservoirs. In this study, natural cores of the Daqing Oilfield were used as the research objects. The throat radius distributions of the different low-permeability cores were determined by the constant velocity mercury injection method, the movable fluid distribution characteristics were determined by nuclear magnetic resonance, and the nonlinear fluid flow characteristics were analyzed via fluid flow experimentation. From these data, the development potential for low-permeability reservoirs was determined. The results show that when the permeability is $1 \times 10^{-3}\ \mu m^2$, the average throat radius is only approximately 0.9 μm and throats with radii less than 0.1 μm account for approximately 30% of the throats. The throats with an average radius less than 1 μm, especially throats with radii less than 0.1 μm, are the main factor restricting the fluid flow in these cores. The movable fluid is only approximately 20% of the fluid in a core, and the threshold pressure gradient reaches 0.15 MPa/m when the permeability is $1 \times 10^{-3}\ \mu m^2$, indicating that it is more difficult to develop reservoirs with permeabilities less than $1 \times 10^{-3}\ \mu m^2$.

1. Introduction

In petroleum reservoirs, the maximum oil recovery due to natural drive mechanisms is only 20%-60%; thus, nearly 9.8×10^{11} t of crude oil is being targeted by various enhanced oil recovery methods [1]. Chemical flooding is mainly adopted to increase oil production in high-permeability reservoirs [2, 3]. The reserves of low-permeability reservoirs are quite large and the main source of oil production [4, 5]. Using China as an example, the reserves of low-permeability reservoirs account for approximately 46% of the total reserves [6]. However, it is very risky and difficult to develop low-permeability reservoirs [7–9]. Taking the low-permeability reservoirs in the Daqing Oilfield as an example, the average daily oil production of each well is 1.2 t/d, and the predicted recovery efficiency is only approximately 15%. The main factor leading to the poor recovery efficiency of low-permeability reservoirs is the complexity of the corresponding fluid flow characteristics [10]. Due to the very small pores and throats and complex pore structure of low-permeability reservoirs, their fluid flow characteristics are nonlinear [11]. The complex flow characteristics are mainly manifested in the following three aspects: first, low-permeability reservoirs exhibit microscale effects. The reservoir rocks are tight, and the average throat radius distribution ranges from 0.2 to 1 μm [12, 13] (far less than that of a high-permeability reservoir [14, 15]). The Jiamin effect can be clearly observed in low-permeability reservoirs due to the distribution of small throat radii [16, 17], leading to a considerable resistance to fluid flow [18]. Second, there is a boundary layer of crude oil on the inner surface of rock pores in low-permeability reservoirs [19, 20]. The composition and properties of the crude oil in this boundary layer are very different from those in the center of the pore [21, 22]. When the pore and throat radius is smaller, the fluid requires more pressure to flow, and the reservoir is more difficult to develop [23, 24]. Third, with the decrease in permeability, the threshold pressure gradient

Table 1: The ionic compositions of the injection water and formation water.

Simulated water	Cation concentration ($mg \cdot L^{-1}$)			Anion concentration ($mg \cdot L^{-1}$)			Salinity ($mg \cdot L^{-1}$)
	$Na^+ + K^+$	Ca^{2+}	Mg^{2+}	HCO^{3-}	Cl^-	SO_4^{2-}	
Injection water	28.3	64.1	21.9	350.0	8.9	11.5	484.7
Formation water	2013.9	116.2	19.5	1034.9	2559.5	14.4	5758.4

increases sharply in low-permeability reservoirs [25, 26]. Crude oil requires more pressure to flow into small pores and small throats [27]. Above all, the saturation of movable fluid is quite low in low-permeability reservoirs, ranging from 25% to 35% [28, 29], and oil-water diffusion zones are small. The recovery efficiency of water flooding is quite low in low-permeability reservoirs [30, 31]. Currently, little research has been performed to determine the development potential for low-permeability reservoirs, which limits their development. Some studies have been performed considering fluid mechanics in porous media and reservoir engineering principles [32–34], but no enough experimental data are available to validate the accuracy of the formulas. For the development of low-permeability reservoirs to be less risky and more efficient, it is important to determine the development potential of low-permeability reservoirs. In this paper, the natural cores of the Daqing Oilfield were taken as the research objects. The throat radius distribution, movable fluid distribution characteristics, and threshold pressure gradient were determined for different low-permeability cores. This information, combined with the observed pore and fluid flow characteristics, was used to determine the development potential of low-permeability reservoirs. The results can provide theoretical guidance for decisions that are made during the development of low-permeability reservoirs.

2. Materials and Methods

2.1. Experimental Materials. The natural cores were chosen from the Fuyang layer of the Daqing Oilfield. The Daqing oil is in the sandstone reservoir, and fluvial facies and delta plain facies are the main sedimentary facies of the Fuyang layer. One hundred ten natural cores were taken from the Fuyang layer, with porosities ranging from 12.40% to 17.75% and permeabilities ranging from $0.36 \times 10^{-3}\ \mu m^2$ to $14.82 \times 10^{-3}\ \mu m^2$. The simulated oil was prepared from wellhead crude oil and aviation kerosene with a viscosity of 6.0 mPa·s at 45°C. The ionic compositions of the injection water and formation water are shown in Table 1.

2.2. Experimental Methods

2.2.1. Throat Radius Measurement. An ASPE730 constant speed mercury injection apparatus was used to measure the throat radius of the different low-permeability cores. The inlet mercury pressure was approximately 6.89 MPa, and the inlet mercury speed was 0.00005 mL/min. The contact angle of the mercury was 140°, and the interfacial tension of the mercury was 485 dyne/cm [35].

2.2.2. Threshold Pressure Gradient Measurement

(1) The natural cores were washed with benzene solution to remove the crude oil

(2) The cores were vacuumed with a vacuum pump for at least 24 h and then saturated in simulated formation water

(3) The simulated formation water was injected into the cores at a rate of 0.01 mL/min, and the flow rate and pressure were recorded

(4) The relationship between flow rate and pressure was obtained by gradually increasing the flow rate of the injected water

2.2.3. Measurement of Movable Fluid. A Newmyer MINI-NMR instrument was used as the experimental apparatus. In the experiment, the magnet temperature was set to 32°C, and the field intensity was 0.5 T. The experimental steps are as follows:

(1) The natural cores were washed with benzene solution to remove the crude oil

(2) The core permeabilities were measured using a gas permeability tester

(3) The cores were vacuumed with a vacuum pump for at least 24 h, and they were saturated in simulated formation water under a pressure of 10 MPa. The core weights were measured, and the porosity was calculated

(4) The cores were placed in a magnetic resonance imaging (MRI) analyzer with a low magnetic field for the MRI T_2 test. The T_2 relaxation time spectra were calculated

3. Throat Radii of the Low-Permeability Reservoirs

3.1. Throat Radius Distribution Characteristics. Forty-six natural cores with different permeabilities were chosen for constant velocity mercury injection. A DM4500P polarizing microscope and a JSM-5600LLV scanning electron microscope were used to observe the pore structure, as shown in Figure 1. The throat radius distributions of different low-permeability cores are shown in Figure 2. The proportions of the different types of throats are shown in Figure 3.

The pores and throats are very small in these low-permeability cores, and with decreasing permeability, the

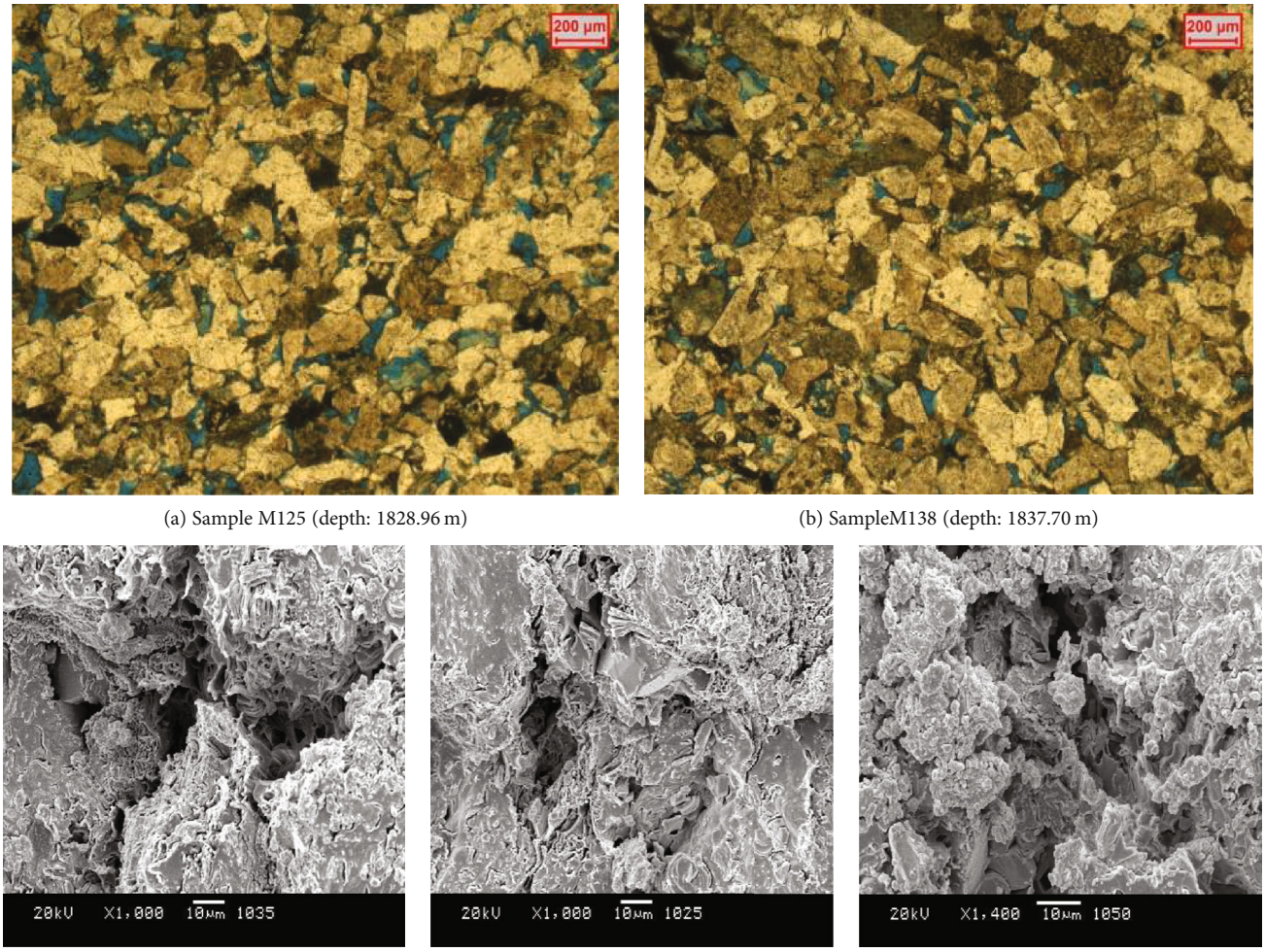

(a) Sample M125 (depth: 1828.96 m)

(b) SampleM138 (depth: 1837.70 m)

(c) Intercrystalline pores

(d) Residual intergranular pore

(e) Tubular throat

Figure 1: Images of pore structure using polarizing microscopy and scanning electron microscopy.

throat radii decrease, making the reservoir more difficult to develop. When the permeability is greater than $10 \times 10^{-3}\ \mu m^2$, most of the throat radii are larger than $1\ \mu m$, accounting for 75.25% of the throats. When the permeability is less than $5 \times 10^{-3}\ \mu m^2$, most of the throat radii are smaller than $1\ \mu m$. When the permeability is between $1 \times 10^{-3}\ \mu m^2$ and $2 \times 10^{-3}\ \mu m^2$, the throat radii are between $0.1\ \mu m$ and $1\ \mu m$, accounting for 61.05% of the throats, while throats with radii less than $0.1\ \mu m$ account for 12.36% of the throats. When the permeability is less than $1 \times 10^{-3}\ \mu m^2$, the number of throats with radii less than $0.1\ \mu m$ increases, accounting for 32.52% of the throats.

3.2. Average Throat Radius Results for the Different Low-Permeability Cores. According to the results of the throat radius distributions for the different low-permeability cores, the average throat radius results were calculated, and the relationship between the average throat radius and permeability is shown in Figure 4.

As shown, when the permeability is greater than $1.13 \times 10^{-3}\ \mu m^2$, the average throat radius is larger than $1\ \mu m$, and the average throat radius increases gradually with increasing permeability. When the permeability is less than $1.13 \times 10^{-3}\ \mu m^2$, the average throat radius is less than $1\ \mu m$, and the average throat radius rapidly decreases as permeability decreases. This indicates that it is more difficult to develop reservoirs with permeabilities less than $1.13 \times 10^{-3}\ \mu m^2$.

4. Movable Fluids in the Low-Permeability Reservoirs

4.1. Movable Fluid Characteristics. Twenty-nine natural cores with different permeabilities were selected from the low-permeability reservoirs, and the magnetic resonance method was used to measure the T_2 spectrum curves. The results show that the T_2 spectrum curve is generally divided into three types: the left peak value is larger than that of the right peak, the two peak values are almost the same, or the right peak value is larger than that of the left peak, as shown in Figure 5.

When the permeability is less than $6.9 \times 10^{-3}\ \mu m^2$, the left peak value increases as permeability decreases, and when

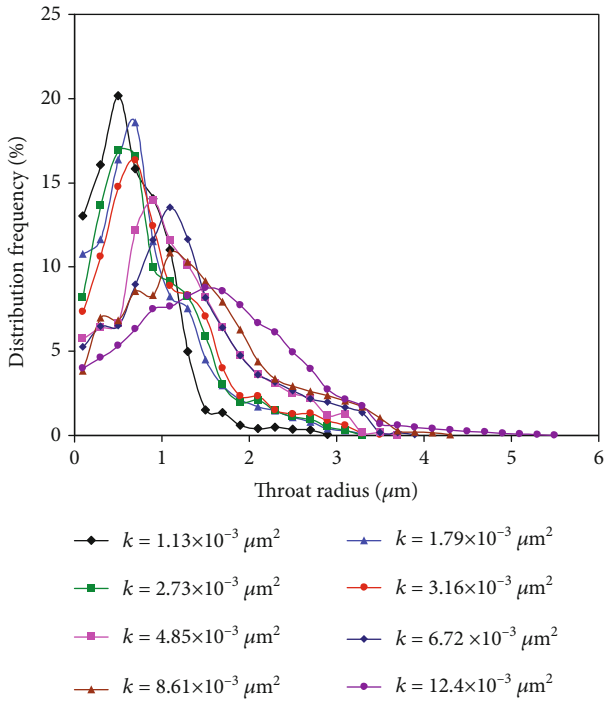

Figure 2: Throat radius distribution of the different low-permeability cores.

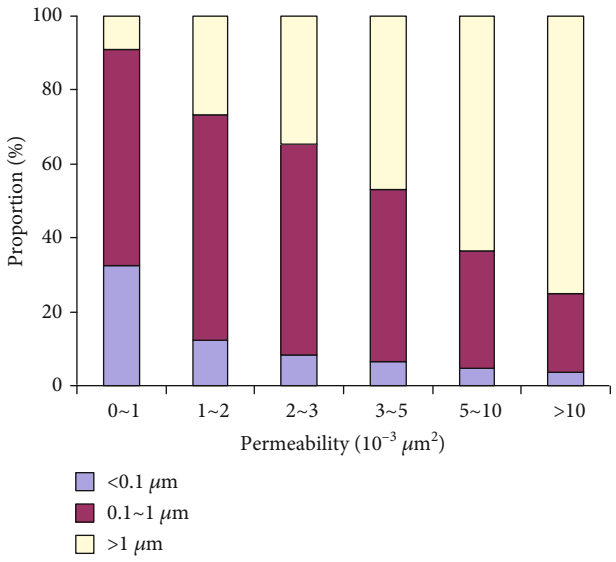

Figure 3: Distribution ratios of the different types of throats in the different low-permeability cores.

the movable fluid percentage decreases, the development potential of the reservoir significantly decreases. When the permeability is approximately 6.9×10^{-3} μm^2, the left and right peak values are almost the same, and the right peak value exceeds the left peak value as permeability further increases. This indicates that the movable fluid percentage

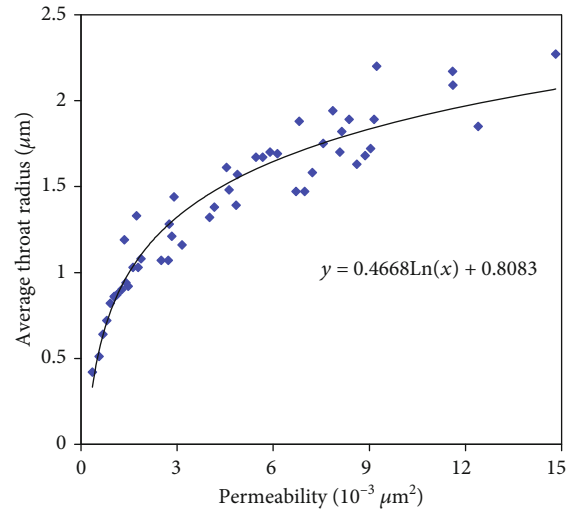

Figure 4: Relationship between permeability and average throat radius.

in the reservoir is high and that the reservoir is feasible for development.

4.2. The Movable Fluid Percentage for the Different Low-Permeability Cores. According to the results of the nuclear magnetic resonance tests, the relationship between movable fluid percentage and permeability is shown in Figure 6.

The relationship of the movable fluid percentage and the permeability is semilogarithmic and similar to the relationship between the permeability and the average throat radius. When the permeability is approximately 5.43×10^{-3} μm^2, the movable fluid percentage is approximately 39.28%. When the permeability is 1.04×10^{-3} μm^2, the movable fluid percentage is 18.32%. When the permeability is approximately 0.43×10^{-3} μm^2, the movable fluid percentage is smaller than 8.03%. This indicates that reservoirs with permeabilities less than 1×10^{-3} μm have very low development potential. When the permeability is less than 1×10^{-3} μm^2, throats with radii less than 0.1 μm account for approximately 30% of the throats, whereas throats with radii between 0.1 μm and 1 μm account for approximately 60% of the throats. Throat radii less than 1 μm, especially throats smaller than 0.1 μm, are the main factor restricting fluid flow in reservoirs. The flow resistance is greater when more throat radii are smaller than 1 μm. For reservoirs with permeabilities less than 1×10^{-3} μm, improving the fluid flow via hydraulic fracturing should be considered [36].

5. Threshold Pressure Gradient of the Low-Permeability Reservoirs

Thirty-five natural cores with different permeabilities were selected, and their threshold pressure gradients were tested. The resulting relationship between fluid flow velocity and displacement pressure gradient is shown in Figure 7. The intersection of the fluid flow velocity and pressure gradient axis is the threshold pressure gradient. The oil well pressure

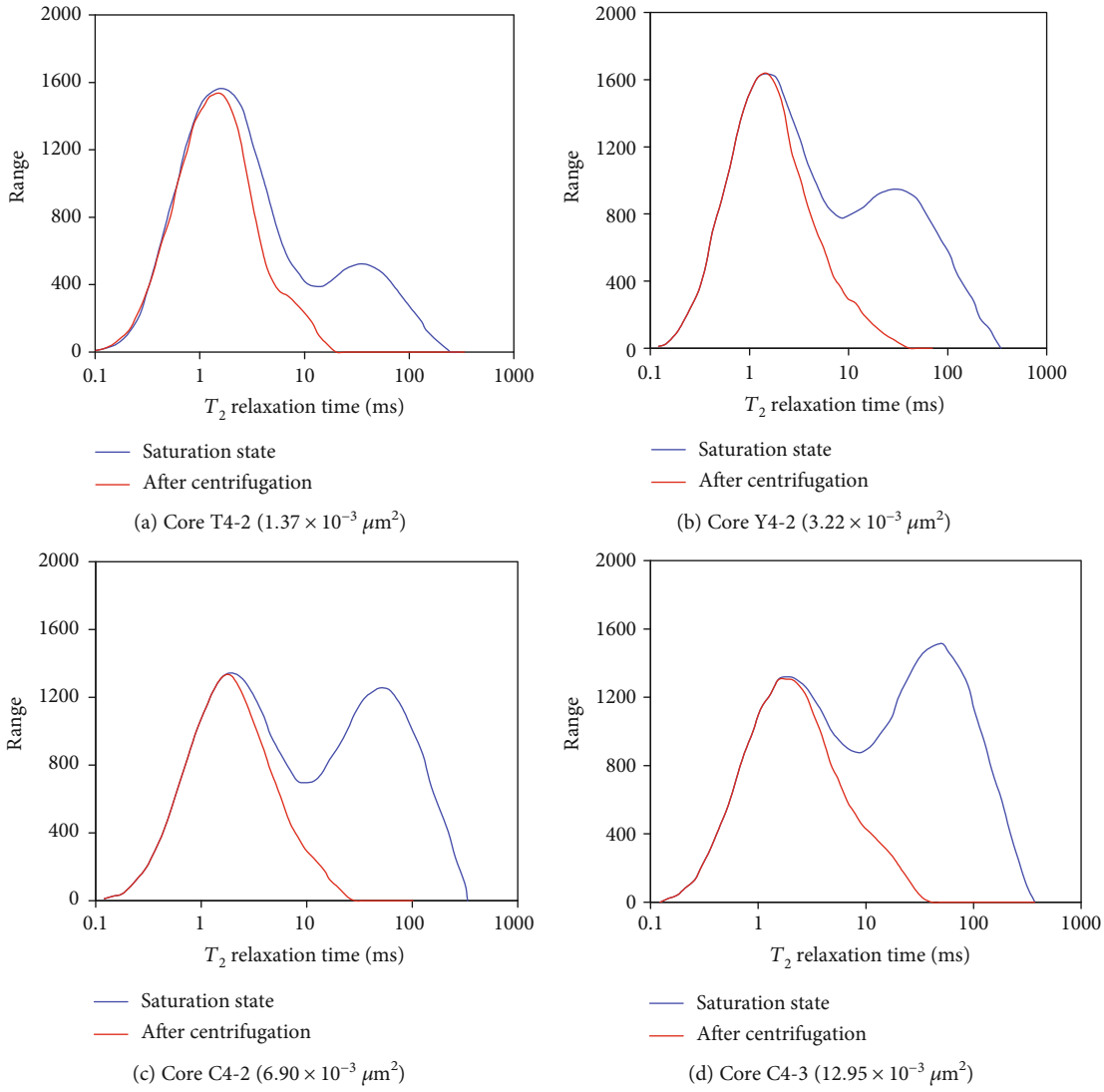

Figure 5: T_2 relaxation time spectra of different low-permeability cores.

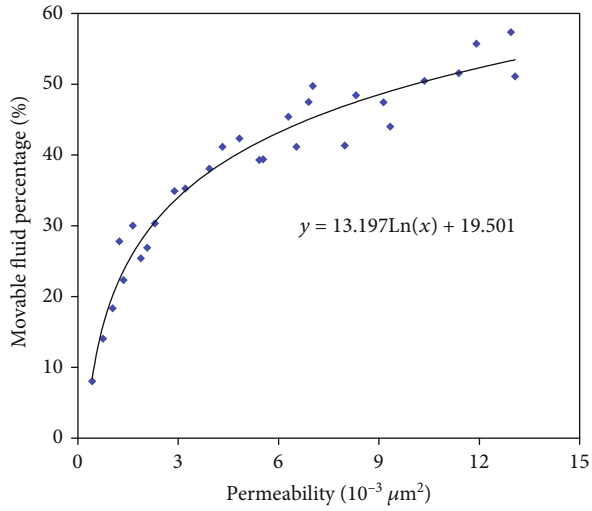

Figure 6: Relationship between movable fluid percentage and permeability.

and water well pressure of 16 oil-producing regions within the Daqing low-permeability reservoir were determined, and the reservoir-scale pressure gradient was calculated by taking the pressure difference between the water well and oil well and dividing by well spacing. The relationship between the threshold pressure gradient and permeability is shown in Figure 8.

The threshold pressure gradient increases as permeability decreases. When the permeability is greater than 1×10^{-3} μm^2, the threshold pressure gradient decreases rapidly as permeability increases. When the permeability is 10.74×10^{-3} μm^2, the threshold pressure gradient is only 0.02 MPa/m. When the permeability is less than 1×10^{-3} μm^2, the threshold pressure gradient increases rapidly as permeability decreases. When the permeability is 1.26×10^{-3} μm^2, the threshold pressure gradient is 0.15 MPa/m. The main reason for this trend is that throats with radii less than 0.1 μm account for 30% of the throats, and the capillary force is large, which restrains fluid flow.

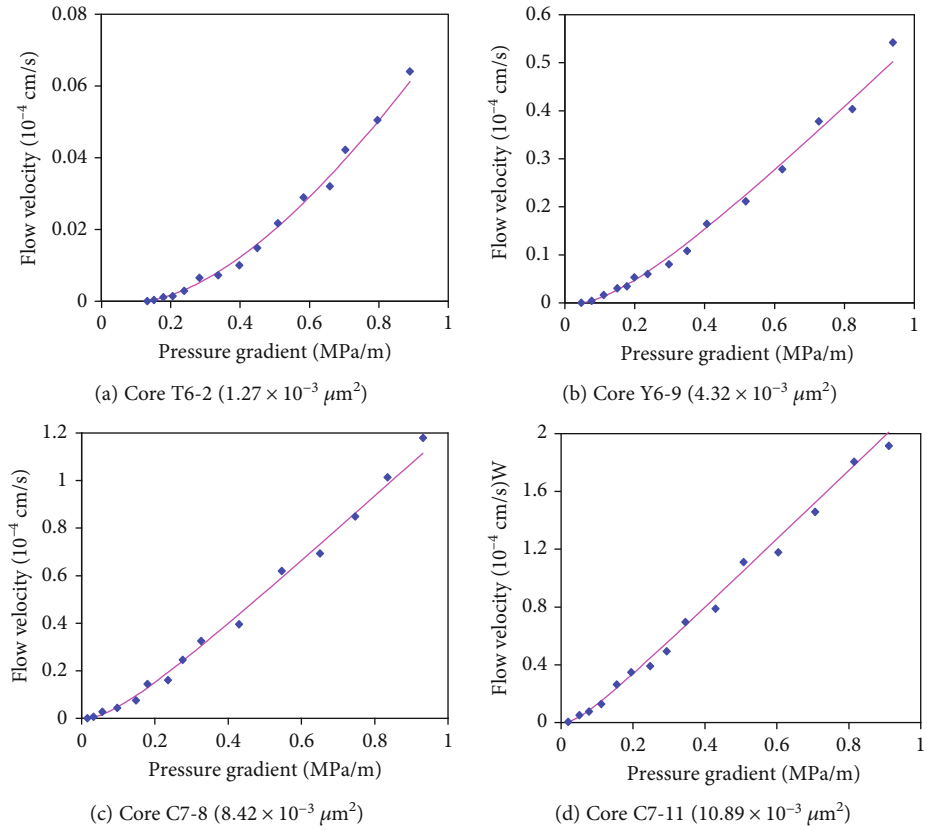

Figure 7: Nonlinear flow curve of different low-permeability cores.

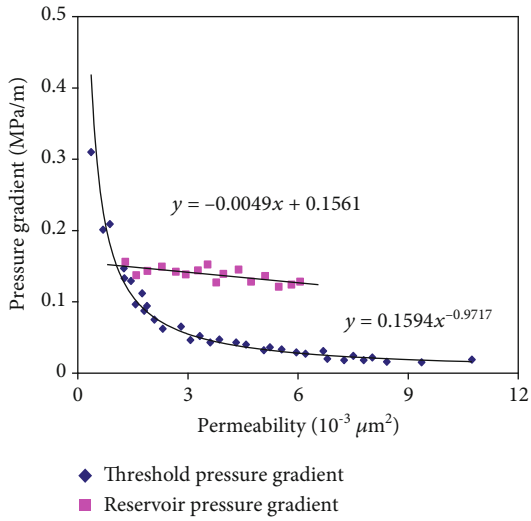

Figure 8: Relationship between permeability and threshold pressure gradient.

There is an intersection point of the reservoir pressure gradient curve and the threshold pressure gradient curve. The permeability at this intersection point is approximately 1×10^{-3} μm^2, which indicates that reservoirs can be successfully developed water injection when the reservoir permeability is greater than 1×10^{-3} μm^2. Additionally, the oil recovery with water flooding is very low when the reservoir permeability is less than 1×10^{-3} μm^2.

6. Conclusions

(1) The presence of throats with radii less than 1 μm, especially those with radii less than 0.1 μm, is the main factor restricting the fluid flow in cores. When the permeability is less than 1.13×10^{-3} μm^2, the average throat radius is less than 1 μm, and the number of throats with radii less than 0.1 μm rapidly increases as permeability decreases

(2) There is little development potential for reservoirs with permeabilities less than 1×10^{-3} μm^2. When the permeability is 1.04×10^{-3} μm^2, the movable fluid percentage is 18.32%, and when the permeability is approximately 0.43×10^{-3} μm^2, the movable fluid percentage is less than 8.03%.

(3) When the permeability is less than 1×10^{-3} μm^2, the threshold pressure gradient rapidly increases with decreasing permeability. When the permeability is 1×10^{-3} μm^2, the threshold pressure gradient increases to 0.15 MPa/m. According to the reservoir pressure gradient and threshold pressure gradient data, the oil recovery with water flooding is very low when the reservoir permeability is less than 1×10^{-3} μm^2

Data Availability

The data used to support the findings of this study are included within the manuscript. The data from Figure 1 to Figure 8 are the data used to support the findings of this study.

Conflicts of Interest

No conflict of interest exists in the submission of this manuscript.

Acknowledgments

This work was supported by the Youth Science Fund Project of Northeast Petroleum University under Grant No. 2017QNJL-02.

References

[1] Y. Zhou, D. Yin, W. Chen, B. Liu, and X. Zhang, "A comprehensive review of emulsion and its field application for enhanced oil recovery," *Energy Science & Engineering*, vol. 7, no. 4, pp. 1046–1058, 2019.

[2] C. Zhang, P. Wang, and G. Song, "Study on enhanced oil recovery by multi-component foam flooding," *Journal of Petroleum Science and Engineering*, vol. 177, pp. 181–187, 2019.

[3] K. Xie, X. Lu, H. Pan et al., "Analysis of dynamic imbibition effect of surfactant in microcracks of reservoir at high temperature and low permeability," *SPE Production & Operations*, vol. 33, no. 3, pp. 596–606, 2018.

[4] K. E. Cawiezel and D. V. S. Gupta, "Successful optimization of viscoelastic foamed fracturing fluids with ultralightweight proppants for ultralow-permeability reservoirs," *SPE Production & Operations*, vol. 25, no. 1, pp. 80–88, 2013.

[5] C. Zhang, P. Wang, G. Song, G. Qu, and J. Liu, "Optimization and evaluation of binary composite foam system with low interfacial tension in low permeability fractured reservoir with high salinity," *Journal of Petroleum Science and Engineering*, vol. 160, pp. 247–257, 2018.

[6] W. Hu, Y. Wei, and J. Bao, "Development of the theory and technology for low permeability reservoirs in China," *Petroleum Exploration and Development*, vol. 45, no. 4, pp. 685–697, 2018.

[7] T. S. Ramakrishnan and M. G. Supp, "Measurement of ultralow permeability," *AICHE Journal*, vol. 62, no. 4, pp. 1278–1293, 2016.

[8] Y. Li, M. Long, J. Tang, M. Chen, and X. Fu, "A hydraulic fracture height mathematical model considering the influence of plastic region at fracture tip," *Petroleum Exploration and Development*, vol. 47, no. 1, pp. 184–195, 2020.

[9] S.-q. Li, L.-s. Cheng, X.-s. Li, and F. Hao, "Nonlinear seepage flow of ultralow permeability reservoirs," *Petroleum Exploration and Development*, vol. 35, no. 5, pp. 606–612, 2008.

[10] D.-z. Ren, W. Sun, H. Huang, J.-x. Nan, and B. Chen, "Determination of microscopic waterflooding characteristics and influence factors in ultralow permeability sandstone reservoir," *Journal of Central South University*, vol. 24, no. 9, pp. 2134–2144, 2017.

[11] H. Dou, S. Y. Ma, C. Y. Zou, and S. L. Yao, "Threshold pressure gradient of fluid flow through multi-porous media in low and extra-low permeability reservoirs," *Science China-earth Sciences*, vol. 57, no. 11, pp. 2808–2818, 2014.

[12] W. Lin, X. Li, Z. Yang et al., "Construction of dual pore 3-D digital cores with a hybrid method combined with physical experiment method and numerical reconstruction method," *Transport in Porous Media*, vol. 120, no. 1, pp. 227–238, 2017.

[13] W. Lin, et al.X. Li, Z. Yang et al., "Multiscale digital porous rock reconstruction using template matching," *Water Resources Research*, vol. 55, no. 8, pp. 6911–6922, 2019.

[14] K. Xie, B. Cao, X. Lu et al., "Matching between the diameter of the aggregates of hydrophobically associating polymers and reservoir pore-throat size during polymer flooding in an offshore oilfield," *Journal of Petroleum Science and Engineering*, vol. 177, pp. 558–569, 2019.

[15] Y. Zhou, D. Wang, Z. Wang, and R. Cao, "The formation and viscoelasticity of pore-throat scale emulsion in porous media," *Petroleum Exploration and Development*, vol. 44, no. 1, pp. 111–118, 2017.

[16] S. F. Shariatpanahi, S. Strand, and T. Austad, "Evaluation of water-based enhanced oil recovery (EOR) by wettability alteration in a low-permeable fractured limestone oil reservoir," *Energy & Fuels*, vol. 24, no. 11, pp. 5997–6008, 2010.

[17] H. Li, Y. Li, S. Chen, J. Guo, K. Wang, and H. Luo, "Effects of chemical additives on dynamic capillary pressure during waterflooding in low permeability reservoirs," *Energy & Fuels*, vol. 30, no. 9, pp. 7082–7093, 2016.

[18] B. Zeng, L. Cheng, and C. Li, "Low velocity non-linear flow in ultra-low permeability reservoir," *Journal of Petroleum Science and Engineering*, vol. 80, no. 1, pp. 1–6, 2011.

[19] J. Wu, L. Cheng, C. Li et al., "Experimental study of nonlinear flow in micropores under low pressure gradient," *Transport in Porous Media*, vol. 119, pp. 247–265, 2017.

[20] W. Liu, J. Yao, Z. Chen, and W. Zhu, "An exact analytical solution of moving boundary problem of radial fluid flow in an infinite low-permeability reservoir with threshold pressure gradient," *Journal of Petroleum Science and Engineering*, vol. 175, no. 175, pp. 9–21, 2019.

[21] X. Wang, Z. Yang, Y. Qi, and Y. Huang, "Effect of absorption boundary layer on nonlinear flow in low permeability porous media," *Journal of Central South University of Technology*, vol. 18, no. 4, pp. 1299–1303, 2011.

[22] Q. Y. Xu, X. G. Liu, and Z. M. Yang, "Nonlinear seepage numerical simulation for super-low permeability reservoirs with artificial fractures," *Petroleum Science and Technology*, vol. 31, no. 1, pp. 23–31, 2013.

[23] L. Zhang, J. Zhang, Y. Wang et al., "Experimental investigation of low-salinity water flooding in a low-permeability oil reservoir," *Energy & Fuels*, vol. 32, no. 3, pp. 3108–3118, 2018.

[24] C. R. Clarkson, A. Vahedian, A. Ghanizadeh, and C. Song, "A new low-permeability reservoir core analysis method based on rate-transient analysis theory," *Fuel*, vol. 235, pp. 1530–1543, 2019.

[25] D. Xu, et al.B. Bai, H. Wu et al., "Mechanisms of imbibition enhanced oil recovery in low permeability reservoirs: effect of IFT reduction and wettability alteration," *Fuel*, vol. 244, pp. 110–119, 2019.

[26] L. Chen, X. Zhu, L. Wang, H. Yang, D. Wang, and M. Fu, "Experimental study of effective amphiphilic graphene oxide flooding for an ultralow-permeability reservoir," *Energy & Fuels*, vol. 32, no. 11, pp. 11269–11278, 2018.

[27] B. Su, J. Yu, S. Liu, and J. Zhang, "Pseudo-percolation threshold theory in evaluation of low-porosity and low-permeability oil reservoir," *Energy Exploration & Exploitation*, vol. 32, no. 4, pp. 621–633, 2014.

[28] D. Wang, D. Yin, and X. Gong, "Numerical simulation of microemulsion flooding in low-permeability reservoir," *Journal of Chemistry*, vol. 2019, Article ID 5021473, 8 pages, 2019.

[29] W. Dongqi, Y. Daiyin, and Z. Yazhou, "Fine classification of ultra-low permeability reservoirs around the Placanticline of Daqing oilfield (PR of China)," *Journal of Petroleum Science and Engineering*, vol. 174, pp. 1042–1052, 2019.

[30] G. Gutierrez Murillo, J. Avendano Rodriguez, J. Saguero Centeno, E. Medina, and A. Perez, "Application of concepts to improve oil production in low-permeability turbidite reservoirs in Mexico," in *SPE Latin America and Caribbean Petroleum Engineering Conference Society of Petroleum Engineers*, pp. 228–238, Maracaibo, Venezuela, May 2014.

[31] Y. Li, Z. Rui, W. Zhao et al., "Study on the mechanism of rupture and propagation of T-type fractures in coal fracturing," *Journal of Natural Gas Science and Engineering*, vol. 52, pp. 379–389, 2018.

[32] T. A. Blasingame, "The characteristic flow behavior of low-permeability reservoir systems," in *SPE Unconventional Reservoirs Conference Society of Petroleum Engineers*, pp. 148–178, Keystone, Colorado, USA, February2008.

[33] S. Selemenev, A. Vasiliev, M. Kolesova, and A. Shekian, "Integrated Perspective Assessment for Complex Low-Permeability Reservoir," in *SPE Russian Oil and Gas Technical Conference and Exhibition Society of Petroleum Engineers*, Moscow, Russia, October 2008.

[34] K. W. Shanley and R. M. Cluff, "The evolution of pore-scale fluid-saturation in low-permeability sandstone reservoirs," *AAPG Bulletin*, vol. 99, no. 10, pp. 1957–1990, 2015.

[35] H. Wu, R. Liu, Y. Ji et al., "Fractal characteristics of pore-throat of tight gas reservoirs and its relation with percolation:a case from the 8 member of the Permian Xiashihezi formation in Ordos Basin," *Acta Sedimentologica Sinica*, vol. 1, pp. 151–162, 2017.

[36] Y. Li, S. Yang, W. Zhao, W. Li, and J. Zhang, "Experimental of hydraulic fracture propagation using fixed-point multistage fracturing in a vertical well in tight sandstone reservoir," *Journal of Petroleum Science and Engineering*, vol. 171, pp. 704–713, 2018.